

Sinkformers: Transformers with Doubly Stochastic Attention

Michael E. Sander
ENS and CNRS

Pierre Ablin
ENS and CNRS

Mathieu Blondel
Google Research, Brain team

Gabriel Peyré
ENS and CNRS

Abstract

Attention based models such as Transformers involve pairwise interactions between data points, modeled with a learnable attention matrix. Importantly, this attention matrix is normalized with the SoftMax operator, which makes it row-wise stochastic. In this paper, we propose instead to use Sinkhorn’s algorithm to make attention matrices doubly stochastic. We call the resulting model a Sinkformer. We show that the row-wise stochastic attention matrices in classical Transformers get close to doubly stochastic matrices as the number of epochs increases, justifying the use of Sinkhorn normalization as an informative prior. On the theoretical side, we show that, unlike the SoftMax operation, this normalization makes it possible to understand the iterations of self-attention modules as a discretized gradient-flow for the Wasserstein metric. We also show in the infinite number of samples limit that, when rescaling both attention matrices and depth, Sinkformers operate a heat diffusion. On the experimental side, we show that Sinkformers enhance model accuracy in vision and natural language processing tasks. In particular, on 3D shapes classification, Sinkformers lead to a significant improvement.

1 Introduction

The Transformer (Vaswani et al., 2017), an architecture that relies entirely on attention mechanisms (Bahdanau et al., 2014), has achieved state of the art empirical success in natural language processing (NLP) (Brown et al., 2020; Radford et al., 2019; Wolf

et al., 2019) as well as in computer vision (Dosovitskiy et al., 2020; Zhao et al., 2020; Zhai et al., 2021; Lee et al., 2019). As the key building block of the Transformer, the self-attention mechanism takes the following residual form (Yun et al., 2019) given a n -sequence (x_1, x_2, \dots, x_n) , embedded in dimension d :

$$x_i \leftarrow x_i + \sum_{j=1}^n K_{i,j}^1 W_V x_j, \quad (1)$$

where $K^1 := \text{SoftMax}(C)$ with $C_{i,j} := (W_Q x_i)^\top W_K x_j = x_i^\top W_Q^\top W_K x_j$. Here, $W_Q, W_K \in \mathbb{R}^{m \times d}$ and $W_V \in \mathbb{R}^{d \times d}$ are the query, key and value matrices. The SoftMax operator can be seen as a normalization of the matrix $K^0 := \exp(C)$ as follows: $K_{i,j}^1 := K_{i,j}^0 / \sum_{l=1}^n K_{i,l}^0$ for all i and j . Importantly, the matrix K^1 is row-wise stochastic: its rows all sum to 1.

In this work, we propose to take the normalization process further by successively normalizing the rows and columns of K^0 . This process is known to provably converge to a doubly stochastic matrix (i.e., whose rows and columns both sum to 1) and is called Sinkhorn’s algorithm (Sinkhorn, 1964; Cuturi, 2013; Peyré et al., 2019). We denote the resulting doubly stochastic matrix K^∞ . Intuitively, such a normalization relies on a democratic principle where all points are matched one to another with different degrees of intensity, so that more interactions are considered than with the SoftMax normalization, as shown in Figure 1.

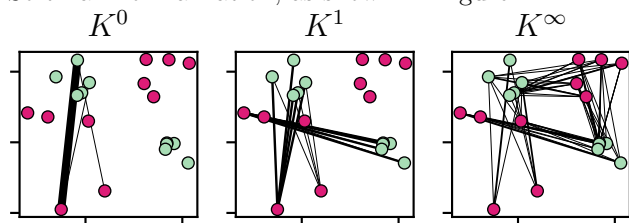


Figure 1: **Illustration of the different normalizations of attention matrices.** We form two point clouds $(W_Q x_i)_{1 \leq i \leq 10}$ (green) and $(W_K x_j)_{1 \leq i \leq 10}$ (red). For $k \in \{0, 1, \infty\}$, the width of the line connecting x_i to x_j is $K_{i,j}^k$. We only display connections with $K_{i,j}^k \geq 10^{-12}$. For K^0 , one interaction dominates. For K^1 (SoftMax), one cluster is ignored. For K^∞ (Sinkhorn), all points are involved in an interaction.

We call our Transformer variant where the SoftMax is replaced by Sinkhorn a **Sinkformer**. Since Sinkhorn’s first iteration coincides exactly with the SoftMax, Sinkformers include Transformers as a special case. Our modification is differentiable, easy to implement using deep learning libraries, and can be executed on GPUs for fast computation. Because the set of row-wise stochastic matrices contains the set of doubly stochastic matrices, the use of doubly stochastic matrices can be interpreted as a prior. On the experimental side, we confirm that doubly stochastic attention leads to better accuracy in several learning tasks. On the theoretical side, doubly stochastic matrices also give a better understanding of the mathematical properties of self-attention maps.

To summarize, we make the following contributions.

- We show empirically that row-wise stochastic matrices seem to converge to doubly stochastic matrices during the learning process in several classical Transformers (Figure 2). Motivated by this finding, we then introduce the Sinkformer, an extension of the Transformer in which the SoftMax is replaced by the output of Sinkhorn’s algorithm. In practice, our model is parametrized by the number of iterations in the algorithm, therefore interpolating between the Transformer and the Sinkformer.
- On the theoretical side, we show that Transformers and Sinkformers can be viewed as models acting on discrete distributions, and we show under a symmetry assumption that Sinkformers can be seen in the infinite depth limit as a Wasserstein gradient flow for an energy minimization (Proposition 2). We also show that the classical Transformer with the SoftMax operator cannot be interpreted as such a flow (Proposition 3). To the best of our knowledge, this is the first time such a connection is established. We also prove that in the infinite number of particles limit (when n goes to infinity), the iterations of Sinkformers converge to the heat equation (Theorem 1), while the corresponding equation for Transformers is nonlinear and nonlocal (Proposition 4).
- On the experimental side, we show that Sinkformers lead to a significant accuracy gain compared to Transformers on the ModelNet 40 3D shapes classification task. We then demonstrate better performance of Sinkformers on the NLP IMDb dataset for sentiment analysis and IWSLT’14 German to English neural machine translation tasks. Sinkformers also achieve a better accuracy than Vision Transformers on image classification tasks. Therefore, the proposed method is capable of enhancing the performance of transformers in a wide range of applications.

2 Background and related work

Transformers. Proposed by Vaswani et al. (2017), the Transformer is a fully attention-based architecture. Originally designed to process sequences for natural language processing (NLP), many variants have since been developed such as Vision Transformers (Dosovitskiy et al., 2020; Zhai et al., 2021), Set Transformers (Lee et al., 2019) or Point Cloud Transformers (Zhao et al., 2020). The Transformer and its variants are based on an encoder-decoder structure, where the decoder can have a more or less complex form. The encoder is fully *self*-attention based. After embedding and concatenating with positional encoding the original input sequence, the encoder uses a series of residual blocks that iterates relation (1) followed by a feed forward neural network applied to each x_i independently. In its most complex form such as in neural machine translation, the decoder combines a self-attention based mechanisms and a *cross* attention one, meaning that it is given access to the encoder via another multi-head attention block.

Sinkhorn and Attention. To the best of our knowledge, using Sinkhorn’s algorithm in Transformers has been done once in a different context (Tay et al., 2020). The authors propose to learn efficient and sparse attention using a differentiable algorithm for sorting and rearranging elements in the input sequence. For this purpose, they introduce a sorting network to generate a doubly-stochastic matrix (that can be seen as a relaxed version of a permutation matrix) and use it to sort the sequence in a differentiable fashion. Mialon et al. (2021) propose an embedding for sets of features in \mathbb{R}^d based on Sinkhorn’s algorithm, by using the regularized optimal transport plan between data points and a reference set. Niculae et al. (2018) use doubly stochastic attention matrices in LSTM-based encoder-decoder networks but they use Frank-Wolfe or active set methods to compute the attention matrix. None of these works use Sinkhorn on self-attention maps in Transformers and provide its theoretical analysis, as we do.

Impact of bi-normalization. Theoretical properties of kernels \mathcal{K} , which attention is an instance of, can also be studied through the operator $f \mapsto f - \mathcal{K}f$. Bi-normalization of kernels over manifolds have already been studied in the literature, on uniform measures (Singer, 2006), weighted measures (Hein et al., 2007) and in a more general setup with associated diffusion operators (Ting et al., 2011). Milanfar (2013) proposes to approximate smoothing operators by doubly stochastic matrices using Sinkhorn’s updates, leading to better performance in data analysis and signal pro-

cessing. Importantly, the works of Marshall and Coifman (2019) and Wormell and Reich (2021) exactly introduce a normalization that is based on Sinkhorn’s algorithm. They prove that this method models a Langevin diffusion and leads to the approximation of a symmetric operator. They also show that convergence to this operator is faster with Sinkhorn normalization than with the SoftMax normalization. In section 5, we adopt a similar point of view with a parametrized cost and show that different normalizations result in different partial differential equations (PDEs) in the infinite number of particles limit.

Infinite depth limit. Studying deep residual neural networks (ResNets) (He et al., 2016) in the infinitesimal step-size regime (or infinite depth limit) has recently emerged as a new framework for analyzing their theoretical properties. The ResNet equation

$$x_i \leftarrow x_i + T(x_i) \quad (2)$$

can indeed be seen as a discretized Euler scheme with unit step size of the ordinary differential equation (ODE) $\dot{x}_i = T(x_i)$ (Weinan, 2017; Chen et al., 2018; Teh et al., 2019; Sun et al., 2018; Weinan et al., 2019; Lu et al., 2018; Ruthotto and Haber, 2019; Sander et al., 2021). In section 4, we adopt this point of view on residual attention layers in order to get a better theoretical understanding of attention mechanisms. This is justified by the fact that, for instance, GPT-3 (Brown et al., 2020) has 96 layers.

Neural networks on measures. The self-attention mechanism (1) acts on sets $\{x_i\}_i$ where the ordering of the elements does not matter. An equivalent way to model such invariant architectures is to consider them as acting on probability measures or point clouds of varying cardinality (De Bie et al., 2019; Vuckovic et al., 2021; Zweig and Bruna, 2021). Specifically, a collection of points $(x_i)_{1 \leq i \leq n}$, where $x_i \in \mathbb{R}^d$, can also be seen as a discrete measure on \mathbb{R}^d : $\mu := \frac{1}{n} \sum_{i=1}^n \delta_{x_i} \in \mathcal{M}(\mathbb{R}^d)$, where $\mathcal{M}(\mathbb{R}^d)$ is the set of probability measures on \mathbb{R}^d . A map T_μ then acts on μ through $F(\mu) := \frac{1}{n} \sum_{i=1}^n \delta_{T_\mu(x_i)}$. One notable interest of such a point of view is to consider the evolution of non ordered sets of points. Another is to consider the mean field (or large sample) limit, that is when $n \rightarrow \infty$, to conduct theoretical analysis (Zweig and Bruna, 2021) as when analyzing the SGD properties in the mean-field limit (Song et al., 2018).

3 Sinkformers

We now introduce Sinkformers, a modification of any Transformer by replacing the SoftMax operator in the attention modules by Sinkhorn’s algorithm.

Attention matrices during training. In Transformers, attention matrices are row-wise stochastic. A natural question is how the sum over columns evolve during training. On 3 different models and 3 different learning tasks, we calculated the sum over columns of attention matrices in Transformers. We find out that the learning process makes the attention matrices more and more doubly stochastic, as shown in Figure 2.

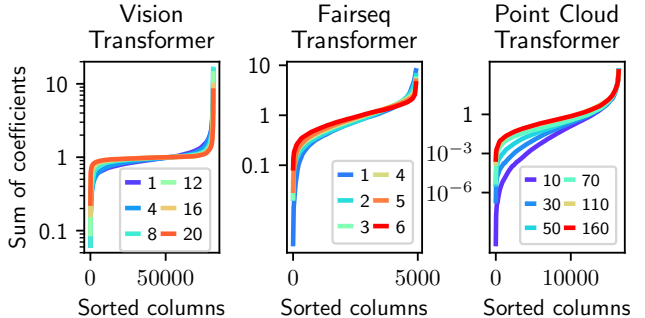


Figure 2: **Sum over columns** of attention matrices at different training epochs (color) when training, from left to right, a ViT on MNIST (section 6.4), a fairseq Transformer on IWSLT’14 (section 6.3), and a Point Cloud Transformer on Model Net 40 (section 6.1). **The majority of columns naturally sum closely to 1.**

Thus, row-wise stochastic attention matrices seem to approach doubly stochastic matrices during the learning process in classical Transformers. Therefore, it seems natural to impose double stochasticity as a prior and study theoretically and experimentally the resulting model. A process to obtain such matrices which extends the SoftMax is Sinkhorn’s algorithm.

Sinkhorn’s algorithm. Given a matrix $C \in \mathbb{R}^{n \times n}$, and denoting $K^0 \in \mathbb{R}^{n \times n}$ such that $K^0 = \exp(C)$, Sinkhorn’s algorithm (Sinkhorn, 1964; Cuturi, 2013; Peyré et al., 2019) iterates, starting from K^0 :

$$K^{l+1} = \begin{cases} N_R(K^l) & \text{if } l \text{ is even} \\ N_C(K^l) & \text{if } l \text{ is odd,} \end{cases} \quad (3)$$

where N_R and N_C correspond to row-wise and column-wise normalizations: $(N_R(K))_{i,j} := \frac{K_{i,j}}{\sum_{l=1}^n K_{i,l}}$ and $(N_C(K))_{i,j} := \frac{K_{i,j}}{\sum_{l=1}^n K_{l,j}}$. We denote the resulting scaled matrix limit $K^\infty := \text{Sinkhorn}(C)$. Note that it is doubly stochastic in the sense that $K^\infty \mathbf{1}_n = \mathbf{1}_n$ and $K^\infty{}^\top \mathbf{1}_n = \mathbf{1}_n$. The operations in (3) are perfectly suited for being executed on GPUs (Charlier et al., 2021; Cuturi, 2013).

Sinkformers. For simplicity, we consider a one head attention block that iterates equation (1). Note that $K^1 := \text{SoftMax}(C)$ is precisely the output of Sinkhorn’s algorithm (3) after 1 iteration. In this

paper, we propose to take Sinkhorn’s algorithm several steps further until it approximately converges to a doubly stochastic matrix K^∞ . This process can be easily implemented in practice, simply by plugging Sinkhorn’s algorithm into self-attention modules in existing architectures, without changing the overall structure of the network. We call the resulting drop-in replacement of a Transformer a Sinkformer. It iterates

$$x_i \leftarrow x_i + \sum_{j=1}^n K_{i,j}^\infty W_V x_j. \quad (4)$$

In the next two sections 4 and 5, we investigate the theoretical properties of Sinkformers. We exhibit connections with energy minimization in the space of measures and the heat equation, thereby proposing a new framework for understanding attention mechanisms. All our experiments are described in Section 6 and show the benefits of using Sinkformers in a wide variety of applications.

Computational cost and differentiation. Turning a Transformer into a Sinkformer simply relies on replacing the SoftMax by Sinkhorn, i.e., substituting K^1 with K^∞ . In practice, we use a finite number of Sinkhorn iterations and therefore use K^l , where l is large enough so that K^l is almost doubly stochastic. Doing l iterations of Sinkhorn takes l times longer than the SoftMax. However, this is not a problem in practice because Sinkhorn is not the main computational bottleneck and because only a few iterations of Sinkhorn are sufficient (typically 3 to 5) to converge to a doubly stochastic matrix. As a result, the practical training time of Sinkformers is comparable to regular Transformers, as detailed in our experiments.

Sinkhorn is perfectly suited for backpropagation (automatic differentiation), by differentiating through the operations of (3). The Jacobian of an optimization problem solution can also be computed using the implicit function theorem (Griewank and Walther, 2008; Krantz and Parks, 2012; Blondel et al., 2021) instead of backpropagation if the number of iterations becomes a memory bottleneck. Together with Sinkhorn, implicit differentiation has been used by Luise et al. (2018) and Cuturi et al. (2020).

Invariance to the cost function. Recall that in practice one has $C_{i,j} = (W_Q x_i)^\top W_K x_j$. An important aspect of Sinkformers is that their output is unchanged if the cost is modified with non interacting terms, as the next proposition shows.

Proposition 1. *Let $C \in \mathbb{R}^{n \times n}$. Consider, for $(f, g) \in \mathbb{R}^n \times \mathbb{R}^n$ the modified cost function $\tilde{C}_{i,j} := C_{i,j} + f_i + g_j$. Then $\text{Sinkhorn}(C) = \text{Sinkhorn}(\tilde{C})$.*

A proof is available in Appendix A. A consequence

of this result is that one can consider the cost $\tilde{C}_{i,j} := -\frac{1}{2} \|W_Q x_i - W_K x_j\|^2$ instead of $C_{i,j} = (W_Q x_i)^\top W_K x_j$, without affecting K^∞ . A Transformer using the cost \tilde{C} is referred to as L2 self-attention, and is Lipschitz under some assumptions (Kim et al., 2021) and can therefore be used as an invertible model (Behrmann et al., 2019). For instance, we use \tilde{C} in Proposition 4.

4 Attention and gradient flows

In this section, we make a parallel between self-attention modules in Sinkformers and gradient flows in the space of measures. We denote $\mathcal{M}(\mathbb{R}^d)$ the probability measures on \mathbb{R}^d and $\mathcal{C}(\mathbb{R}^d)$ the continuous functions on \mathbb{R}^d . We denote ∇ the gradient operator, div the divergence, and Δ the Laplacian, that is $\Delta = \text{div}(\nabla)$.

Residual maps for attention. We consider a one-head attention block operating with different normalizations. We consider the continuous counterparts of the attention matrices seen in the previous section. We denote $c(x, x') := (W_Q x)^\top W_K x'$ and $k^0 := \exp(c)$. For some measure $\mu \in \mathcal{M}(\mathbb{R}^d)$, we define the SoftMax operator on the cost c by $k^1(x, x') = \text{SoftMax}(c)(x, x') := \frac{k^0(x, x')}{\int k^0(x, y) d\mu(y)}$. Similarly, we define Sinkhorn’s algorithm as the following iterations, starting from $k^0 = \exp(c)$:

$$k^{l+1}(x, x') = \begin{cases} \frac{k^l(x, x')}{\int k^l(x, y) d\mu(y)} & \text{if } l \text{ is even} \\ \frac{k^l(x, x')}{\int k^l(y, x) d\mu(y)} & \text{if } l \text{ is odd.} \end{cases}$$

We denote $k^\infty := \text{Sinkhorn}(c)$ the resulting limit. Note that if μ is a discrete measure supported on a n sequence of particles (x_1, x_2, \dots, x_n) , $\mu = \frac{1}{n} \sum_{i=1}^n \delta_{x_i}$, then for all (i, j) , $k^0(x_i, x_j) = K_{i,j}^0$, $k^1(x_i, x_j) = K_{i,j}^1$ and $k^\infty(x_i, x_j) = K_{i,j}^\infty$, so that k^0 , k^1 and k^∞ are indeed the continuous equivalent of the matrices K^0 , K^1 and K^∞ respectively.

Infinitesimal step-size regime. In order to better understand the theoretical properties of attention matrices in Transformers and Sinkformers, we omit the feed forward neural networks acting after each attention block. We consider a succession of attention blocks with tied weights between layers and study the infinite depth limit where the output is given by solving a neural ODE (Chen et al., 2018). In this framework, iterating the Transformer equation (1), the ResNet equation (2) and the Sinkformer equation (4) corresponds to a Euler discretization with step-size 1 of the ODEs

$$\dot{x}_i = T_\mu(x_i) \text{ for all } i,$$

where $x_i(t)$ is the position of x_i at time t . For an arbitrary measure $\mu \in \mathcal{M}(\mathbb{R}^d)$, these ODEs can be

equivalently written as a continuity equation (Renardy and Rogers, 2006)

$$\partial_t \mu + \operatorname{div}(\mu T_\mu) = 0. \quad (5)$$

When T_μ is defined by the ResNet equation (2), $T_\mu = T$ does not depend on μ . It defines an advection equation where the particles do not interact and evolve independently. When T_μ is defined by the Transformer equation (1) or Sinkformer equation (4), T_μ has a dependency in μ and the particles interact: the local vector field depends on the position of the other particles. More precisely we have in this case $T_\mu^1(x) = \int k^1(x, x') W_V x' d\mu(x')$ for the Transformer and $T_\mu^\infty(x) = \int k^\infty(x, x') W_V x' d\mu(x')$ for the Sinkformer. It is easily seen that when μ is discrete we recover the operators in equation (1) and (4).

Wasserstein gradient flows. A particular case of equation (5) is when T_μ is a gradient with respect to the Wasserstein metric W_2 . Let \mathcal{F} be a function on $\mathcal{M}(\mathbb{R}^d)$. As is standard, we suppose that \mathcal{F} admits a first variation at all μ : there exists a function $\frac{\delta \mathcal{F}}{\delta \mu}(\mu)$ such that $\frac{d}{d\varepsilon} \mathcal{F}(\mu + \varepsilon \rho)|_{\varepsilon=0} = \int \frac{\delta \mathcal{F}}{\delta \mu}(\mu) d\rho$ for every perturbation ρ (Santambrogio, 2017). The Wasserstein gradient of \mathcal{F} at μ is then $\nabla_W \mathcal{F}(\mu) := \nabla(\frac{\delta \mathcal{F}}{\delta \mu}(\mu))$. The minimization of \mathcal{F} on the space of measures corresponds to the PDE (5) with $T_\mu = -\nabla_W \mathcal{F}(\mu)$. This PDE can be interpreted as ruling the evolution of the measure μ of particles initially distributed according to some measure μ_0 , for which the positions $x(t)$ follow the flow $\dot{x} = -\nabla_W \mathcal{F}(\mu)(x)$, that minimizes the global energy \mathcal{F} . It corresponds to a steepest descent in Wasserstein space (Jordan et al., 1998). In Proposition 2, we show in the symmetric kernel case that Sinkformers correspond to a Wasserstein gradient flow for some functional \mathcal{F}^∞ , while Transformers do not.

Particular case. An example is when T_μ does not depend on μ and writes $T_\mu = -\nabla E$ where $E : \mathbb{R}^d \rightarrow \mathbb{R}$. Under regularity assumptions, a solution of (5) then converges to a local minimum of E . This fits in the implicit deep learning framework (Bai et al., 2019), where a neural network is seen as solving an optimization problem. A typical benefit of implicit models is that the iterates x_i do not need to be stored during the forward pass of the network because gradients can be calculated using the implicit function theorem: it bypasses the memory storage issue of GPUs (Wang et al., 2018; Peng et al., 2017; Zhu et al., 2017) during automatic differentiation. Another application is to consider neural architectures that include an argmin layer, for which the output is also formulated as the solution of a nested optimization problem (Agrawal et al., 2019; Gould et al., 2016, 2019).

Flows for attention. Our goal is to determine the PDEs (5) defined by the proposed attention maps. We consider the symmetric case, summarized by the following assumption:

Assumption 1. $W_K^\top W_Q = W_Q^\top W_K = -W_V$

Assumption 1 means we consider symmetric kernels (by imposing $W_K^\top W_Q = W_Q^\top W_K$), and that when differentiating $x \mapsto \exp(c(x, x'))$, we obtain $-\exp(c)W_V$. We show that, under this assumption, the PDEs defined by k^0 and k^∞ correspond to Wasserstein gradient flows, whereas it is not the case for k^1 . A particular case of imposing $W_K^\top W_Q = W_Q^\top W_K$ is when $W_Q = W_K$. This equality setting is studied by Kim et al. (2021), where the authors show that it leads to similar performance for Transformers. Since imposing $W_K^\top W_Q = W_Q^\top W_K$ is less restrictive, it seems to be a natural assumption. Imposing $W_Q^\top W_K = -W_V$ is more restrictive, and we detail the expressions for the PDEs associated to k^0, k^1, k^∞ without this assumption in Appendix A. We have the following result.

Proposition 2 (PDEs associated to k^0, k^1, k^∞). *Suppose Assumption 1. Let \mathcal{F}^0 and $\mathcal{F}^\infty : \mathcal{M}(\mathbb{R}^d) \rightarrow \mathbb{R}$ be such that $\mathcal{F}^0(\mu) := \frac{1}{2} \int k^0 d(\mu \otimes \mu)$ and $\mathcal{F}^\infty(\mu) := -\frac{1}{2} \int k^\infty \log(\frac{k^\infty}{k^0}) d(\mu \otimes \mu)$. Then k^0, k^1 and k^∞ respectively generate the PDEs $\frac{\partial \mu}{\partial t} + \operatorname{div}(\mu T_\mu^k) = 0$ with $T_\mu^0 := -\nabla_W \mathcal{F}^0(\mu)$, $T_\mu^1 := -\nabla[\log(\int k^0(\cdot, x') d\mu(x'))]$ and $T_\mu^\infty := -\nabla_W \mathcal{F}^\infty(\mu)$.*

A proof is given in Appendix A. Proposition 2 shows that k^0 and k^∞ correspond to Wasserstein gradient flows. In addition, the PDE defined by k^1 does not correspond to such a flow. More precisely, we have the following result.

Proposition 3 (The SoftMax normalization does not correspond to a gradient flow). *One has that $T_\mu^1 = -\nabla[\log(\int k^0(\cdot, x') d\mu(x'))]$ is not a Wasserstein gradient.*

A proof is given in Appendix A, based on the lack of symmetry of T_μ^1 . As a consequence of these results, we believe this variational formulation of attention mechanisms for Sinkformers (Proposition 2) provides a perspective for analyzing the theoretical properties of attention-based mechanisms in light of Wasserstein gradient flow theory (Santambrogio, 2017). Moreover, it makes it possible to interpret Sinkformers as argmin layers, which is promising in terms of theoretical and experimental investigations, and which is not possible for Transformers, according to Proposition 3.

Our results are complementary to the one of Dong et al. (2021), where the authors show that, **with no skip connections** and without the feed forward neural network acting after each attention block, the output of a Transformer converges doubly exponentially

with depth to a rank-1 matrix. On the contrary, we propose a complementary analysis by taking skip-connections into account, as is standard in Transformers. Precisely because we consider such connections, we end up with very different behaviors. Indeed, as shown in the next section, our analysis reveals that the relative signs for W_K , W_Q and W_V imply very different behavior, such as aggregation or diffusion. The dynamics obtained when considering skip connections are therefore richer than a rank collapse phenomenon.

5 Attention and diffusion

In this section, we use the same notations as in section 4. We consider the mean-field limit, where the measure μ has a density with respect to the Lebesgue measure. We are interested in how the density of particles evolves for an infinite depth self-attention network with tied weights between layers. We consider Assumption 1 and suppose that $W_K^\top W_Q$ is positive semi-definite. For a bandwidth $\varepsilon > 0$, let $k_\varepsilon^\infty = \text{Sinkhorn}(c/\varepsilon)$, that is the attention kernel for the Sinkformer with the cost c/ε . The mapping $T_{\mu,\varepsilon}^\infty : x \mapsto \frac{1}{\varepsilon} \int k_\varepsilon^\infty(x, x') W_V x' d\mu(x')$ corresponds to the continuous version of the Sinkformer where we rescale $W_Q W_K^\top = -W_V$ by ε . To better understand the dynamics of attention, we study the asymptotic regime in which the bandwidth $\varepsilon \rightarrow 0$. In this regime, one can show that $\forall x \in \mathbb{R}^d$, $\varepsilon T_{\mu,\varepsilon}^\infty(x) \rightarrow W_V x$ (details in Appendix A). Thus, to go beyond first order, we study the modified map $\bar{T}_{\mu,\varepsilon}^\infty = T_{\mu,\varepsilon}^\infty - \frac{1}{\varepsilon} W_V$. A natural question is the limit of this quantity when $\varepsilon \rightarrow 0$, and what the PDE defined by this limit is. We have the following theorem.

Theorem 1 (Sinkformer’s PDE). *Let $\mu \in \mathcal{M}(\mathbb{R}^d)$. Suppose that μ is supported on a compact set and has a density $\rho \in \mathcal{C}^3(\mathbb{R}^d)$. Suppose assumption 1 and that $W_K^\top W_Q$ is positive semi-definite. Then one has in L^2 norm as $\varepsilon \rightarrow 0$,*

$$\bar{T}_{\mu,\varepsilon}^\infty \rightarrow \bar{T}_{\mu,0}^\infty := -\frac{\nabla \rho}{\rho}.$$

In this limit, the PDE $\partial_t \rho + \text{div}(\rho \bar{T}_{\mu,0}^\infty) = 0$ rewrites

$$\partial_t \rho = \Delta \rho. \quad (6)$$

A proof is available in Appendix A, making use of Theorem 1 from Marshall and Coifman (2019). We recover in Equation (6) the well-known **heat equation**.

We want to compare this result with the one obtained with the SoftMax normalization. In order to carry a similar analysis, we make use of a Laplace expansion result (Tierney et al., 1989; Singer, 2006). However, the kernel $k_\varepsilon^1 = \text{SoftMax}(c/\varepsilon)$ is not suited for using

Laplace method because it does not always have a limit when $\varepsilon \rightarrow 0$. Thus, we consider the modified cost as in Proposition 1, $\tilde{c}(x, x') = -\frac{\|W_Q x - W_K x'\|^2}{2}$. The kernel $\tilde{k}_\varepsilon^1 = \text{SoftMax}(\tilde{c}/\varepsilon)$, for which we can now apply Laplace expansion result, then corresponds to the L2 self-attention formulation (Kim et al., 2021). Note that thanks to Proposition 1, $\tilde{k}_\varepsilon^\infty = k_\varepsilon^\infty$: Sinkorn’s algorithm will have the same output for both costs. To simplify the expressions derived, we assume that W_Q and W_K are in $\mathbb{R}^{d \times d}$ and are invertible. Similarly to the analysis conducted for Sinkformers, we consider the mapping $T_{\mu,\varepsilon}^1 : x \mapsto \frac{1}{\varepsilon} \int \tilde{k}_\varepsilon^1(x, x') W_V x' d\mu(x')$. When $\varepsilon \rightarrow 0$, we show that $\forall x \in \mathbb{R}^d$, $\varepsilon T_{\mu,\varepsilon}^1(x) \rightarrow -W_Q^\top W_Q x$ (details in Appendix A). Thus, we consider $\bar{T}_{\mu,\varepsilon}^1 = T_{\mu,\varepsilon}^1 + \frac{1}{\varepsilon} W_Q^\top W_Q$. We have the following result.

Proposition 4 (Transformer’s PDE). *Let $\mu \in \mathcal{M}(\mathbb{R}^d)$. Suppose that μ is supported on a compact set and has a density $\rho \in \mathcal{C}^1(\mathbb{R}^d)$. Suppose assumption 1 and that W_Q and W_K are in $\mathbb{R}^{d \times d}$ and are invertible. Then one has $\forall x \in \mathbb{R}^d$,*

$$\bar{T}_{\mu,\varepsilon}^1(x) \rightarrow \bar{T}_{\mu,0}^1(x) := -W_Q^\top W_K^{-1} \frac{\nabla \rho}{\rho} (W_K^{-1} W_Q x).$$

In this limit, the PDE $\partial_t \rho + \text{div}(\rho \bar{T}_{\mu,0}^1) = 0$ rewrites

$$\partial_t \rho = \text{div}(W_Q^\top W_K^{-1} \frac{\nabla \rho}{\rho} (W_K^{-1} W_Q \cdot) \rho) \quad (7)$$

A proof is given in Appendix A. While equation (6) corresponds to the heat equation, equation (7) is different. First, it is nonlinear in ρ . Second, it is nonlocal since the evolution of the density at x depends on the value of this density at location $W_K^{-1} W_Q x$. Note that the linear and local aspect of Sinkformer’s PDE on the one hand, and the nonlinear and nonlocal aspect of Transformer’s PDE on the other hand, remain true without assuming $W_Q^\top W_K = -W_V$ (details in Appendix A).

6 Experiments

We now demonstrate the applicability of Sinkformers on a large variety of experiments with different modalities. We use Pytorch (Paszke et al., 2017) and Nvidia Tesla V100 GPUs. Our code is open-sourced and is available at this address: <https://github.com/michaelsdr/sinkformers>. All the experimental details are given in Appendix C.

Practical implementation. In all our experiments, we use existing Transformer architectures and modify the SoftMax operator in attention modules with Sinkhorn’s algorithm, which we implement in log domain for stability (details in Appendix B).

6.1 ModelNet 40 classification

The ModelNet 40 dataset (Wu et al., 2015) is composed of 40 popular object categories in 3D. Transformers for point clouds and sets have been applied to the ModelNet 40 classification in several works, such as Set Transformers (Lee et al., 2019) or Point Cloud Transformers (Guo et al., 2021).

Set Sinkformers. Set Transformers (Lee et al., 2019) also have an encoder decoder structure with different possibilities for defining attention-based set operations. We propose to focus on the architecture that uses *Induced Self Attention Block* (ISAB), which bypasses the quadratic time complexity of Self Attention Blocks (SAB). More details about this architecture can be found in (Lee et al., 2019). We reproduce the ModelNet 40 classification experiment using 5000 uniformly sampled points for each shape and use a Set Transformer and a Set Sinkformer with two ISAB layers in the encoder and a decoder composed of a SAB and a Pooling by Multihead Attention (PMA) module. While the reported test accuracy is of 87.8% using a Set Transformer, we obtain as our best accuracy when performing 21 iterations of Sinkhorn algorithm within our Sinkformer of 89.1%. Results are summarized in Table 1.

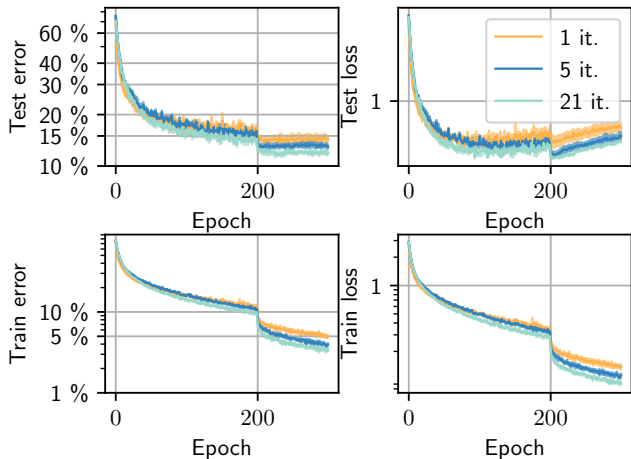


Figure 3: **Classification error and loss on ModelNet 40** when training a Set Transformer and a Set Sinkformer with different number of iterations in Sinkhorn’s algorithm.

Moreover, we show in Figure 3 the learning curves corresponding to this experiment. Interestingly, the number of iterations within Sinkhorn’s algorithm increases the accuracy of the model. Note that we only consider an odd number of iterations since we always want to have row-wise stochastic attention matrices to be consistent with the properties of the SoftMax.

Point Cloud Transformers. We also train Point Cloud Transformers (Guo et al., 2021) on ModelNet 40. This architecture achieves accuracy comparable to the state of the art on this dataset. We compare best and median test accuracy over 4 runs. Results are reported in Table 1, where we see that while the best test-accuracy is narrowly achieved for the Transformer, the Sinkformer has a slightly better median accuracy.

Table 1: **Test accuracy for ModelNet 40** over 4 runs for each model.

Model	Best	Median	Mean	Worst
Set Transformer	87.8%	86.3%	85.8%	84.7%
Set Sinkformer	89.1%	88.4%	88.3%	88.1%
Point Cloud Transformer	93.2%	92.5%	92.5%	92.3%
Point Cloud Sinkformer	93.1%	92.8%	92.7%	92.5%

6.2 Sentiment Analysis

We train a Transformer (composed of an attention-based encoder followed by a max-pooling layer) and a Sinkformer on the IMDB movie review dataset (Maas et al., 2011) for sentiment analysis. This text classification task consists of predicting whether a movie review is positive or negative. The learning curves are shown in Figure 4, with a gain in accuracy when using a Sinkformer. In this experiment, Sinkhorn’s algorithm converges perfectly in 3 iterations (the resulting attention matrices are doubly stochastic), which corresponds to the green curve. The Sinkformer only adds a small computational overhead, since the training time per epoch is 4m 02s for the Transformer against 4m 22s for the Sinkformer.

6.3 Neural Machine Translation

We train a Transformer and its Sinkformer counterpart using the fairseq (Ott et al., 2019) sequence modeling toolkit on the IWSLT’14 German to English dataset (Cettolo et al., 2014). The architecture used is composed of an encoder and a decoder, both of depth 6. We plug Sinkhorn’s algorithm only into the encoder part. Indeed, in the decoder, we can only pay attention to previous positions in the output sequence. For this reason, we need a mask that prevents a straightforward application of Sinkhorn’s algorithm. We demonstrate that even when using the hyper-parameters used to optimally train the Transformer, we achieve a similar BLEU (Papineni et al., 2002) over 6 runs. We first train a Transformer for 30 epochs. On the evaluation set, we obtain a BLEU of 34.43. We then consider a Sinkformer with the weights of the trained Transformer. Interestingly, even this un-adapted Sinkformer provides a median BLEU score of 33.81. We then divide the learning rate by 10 and retrain for 5 additional

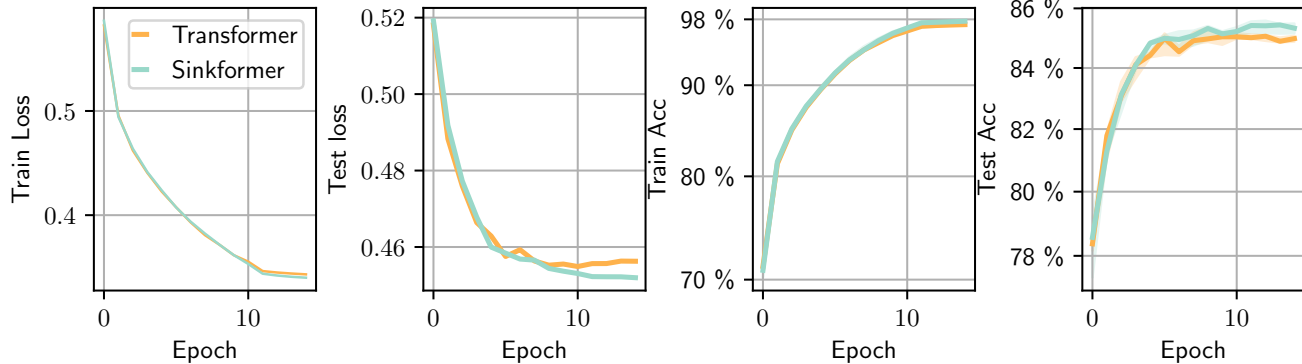


Figure 4: **Learning curves** when training a Transformer and a Sinkformer on the Sentiment Analysis task on the IMDB Dataset.

epochs both the Transformer and the Sinkformer to obtain a median BLEU of respectively 34.68 and 34.73 (Table 2). Importantly, the runtime for one training epoch is almost the same for both models: 2m 48s (Transformer) against 2m 52s (Sinkformer).

Table 2: **Median BLEU score** over 6 runs on the IWSLT’14 German to English dataset. The score * is when evaluating the Sinkformer with the weights of the trained Transformer.

Model	Epoch 30	Epoch 35
Transformer	34.43	34.68
Sinkformer	33.81*	34.73

6.4 Vision Transformers

Vision Transformers (ViT) (Dosovitskiy et al., 2020) have recently emerged as a promising architecture for achieving state of the art performance on computer vision tasks (Zhai et al., 2021), using only attention based mechanisms by selecting patches of fixed size in images and feeding them into an attention mechanism.

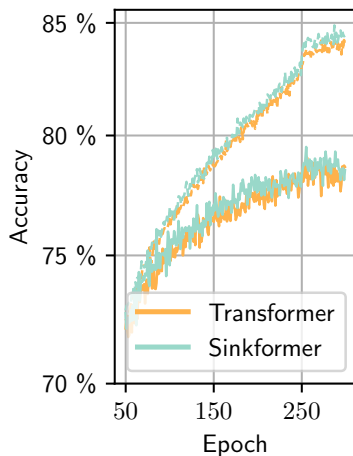


Figure 5: **Train** (dotted) and **test** (plain) **accuracy** as a function of the number of epochs when training a ViT and its Sinkformer counterpart on the cats and dogs classification task (median over 5 runs).

Cats and dogs classification. We train a ViT and its Sinkformer counterpart on a binary cats and dogs image classification task. The evolution of the train and test accuracy is displayed in Figure 5. The *median* test accuracy is 79.0% for the Transformer against 79.5% for the Sinkformer, whereas the *maximum* test accuracy is 80.0% for the Transformer against 80.5% for the Sinkformer. We also use 3 iterations in Sinkhorn’s algorithm which leads to a negligible computational overhead (training time per epoch of 3m 25s for the Sinkformer against 3m 20s for the Transformer).

Impact of the patch size on the final accuracy.

We consider a one-layer and one-head self-attention module on the MNIST dataset, with no additional layer. The purpose is to isolate the self-attention module and study how its accuracy is affected by the choice of the patch size. Results are displayed in Figure 6. We recall that a MNIST image is of size 28×28 . When taking only one patch of size 28, both models are equivalent because the attention matrix is of size 1. However, when the patch size gets smaller, the two models are different and the Sinkformer outperforms the Transformer.

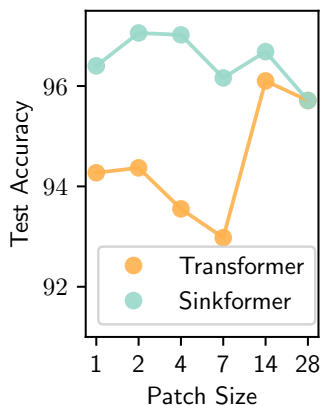


Figure 6: **Final test accuracy** when training a one layer and one head self attention module on the MNIST dataset, with no feedforward neural network, when varying the patch size (median over 5 runs).

Conclusion

In this paper, we presented the Sinkformer, a variant of the Transformer in which the SoftMax, which leads to row-wise stochastic attention, is replaced by Sinkhorn’s algorithm, which leads to doubly stochastic attention. This new model is motivated by the empirical finding that attention matrices in Transformers get closer and closer to doubly stochastic matrices during the training process. This modification is easily implemented in practice by simply replacing the SoftMax in the attention modules of existing Transformers without changing any parameter in the network. It also provides a new framework for theoretically studying attention-based mechanisms, such as the interpretation of Sinkformers as Wasserstein gradient flows in the infinitesimal step size regime or as diffusion operators in the mean-field limit. On the experimental side, Sinkformers lead to better accuracy in a variety of experiments: classification of 3D shapes, sentiment analysis, neural machine translation, and image classification.

Acknowledgments

This work was granted access to the HPC resources of IDRIS under the allocation 2020-[AD011012073] made by GENCI. This work was supported in part by the French government under management of Agence Nationale de la Recherche as part of the “Investissements d’avenir” program, reference ANR19-P3IA-0001 (PRAIRIE 3IA Institute). This work was supported in part by the European Research Council (ERC project NORIA). We thank Marco Cuturi and D. Sculley for their comments on a draft of the paper. We thank Scott Pesme, Pierre Rizkallah, Othmane Sebbouh, Thibault Séjourné and the anonymous reviewers for helpful feedbacks.

References

- Agrawal, A., Amos, B., Barratt, S., Boyd, S., Diamond, S., and Kolter, Z. (2019). Differentiable convex optimization layers. *arXiv preprint arXiv:1910.12430*.
- Bahdanau, D., Cho, K., and Bengio, Y. (2014). Neural machine translation by jointly learning to align and translate. *arXiv preprint arXiv:1409.0473*.
- Bai, S., Kolter, J. Z., and Koltun, V. (2019). Deep equilibrium models. *Advances in Neural Information Processing Systems*, 32:690–701.
- Behrmann, J., Grathwohl, W., Chen, R. T., Duvenaud, D., and Jacobsen, J.-H. (2019). Invertible residual networks. In *International Conference on Machine Learning*, pages 573–582. PMLR.
- Blondel, M., Berthet, Q., Cuturi, M., Frostig, R., Hoyer, S., Llinares-López, F., Pedregosa, F., and Vert, J.-P. (2021). Efficient and modular implicit differentiation. *arXiv preprint arXiv:2105.15183*.
- Brown, T. B., Mann, B., Ryder, N., Subbiah, M., Kaplan, J., Dhariwal, P., Neelakantan, A., Shyam, P., Sastry, G., Askell, A., et al. (2020). Language models are few-shot learners. *arXiv preprint arXiv:2005.14165*.
- Cettolo, M., Niehues, J., Stüker, S., Bentivogli, L., and Federico, M. (2014). Report on the 11th iwslt evaluation campaign, iwslt 2014. In *Proceedings of the International Workshop on Spoken Language Translation, Hanoi, Vietnam*, volume 57.
- Charlier, B., Feydy, J., Glaunès, J., Collin, F.-D., and Durif, G. (2021). Kernel operations on the gpu, with autodiff, without memory overflows. *Journal of Machine Learning Research*, 22(74):1–6.
- Chen, T. Q., Rubanova, Y., Bettencourt, J., and Duvenaud, D. K. (2018). Neural ordinary differential equations. In *Advances in neural information processing systems*, pages 6571–6583.
- Cuturi, M. (2013). Sinkhorn distances: Lightspeed computation of optimal transport. *Advances in neural information processing systems*, 26:2292–2300.
- Cuturi, M., Teboul, O., Niles-Weed, J., and Vert, J.-P. (2020). Supervised quantile normalization for low rank matrix factorization. In *International Conference on Machine Learning*, pages 2269–2279. PMLR.
- De Bie, G., Peyré, G., and Cuturi, M. (2019). Stochastic deep networks. In *International Conference on Machine Learning*, pages 1556–1565. PMLR.
- Dong, Y., Cordonnier, J.-B., and Loukas, A. (2021). Attention is not all you need: Pure attention loses rank doubly exponentially with depth. *arXiv preprint arXiv:2103.03404*.
- Dosovitskiy, A., Beyer, L., Kolesnikov, A., Weissenborn, D., Zhai, X., Unterthiner, T., Dehghani, M., Minderer, M., Heigold, G., Gelly, S., et al. (2020). An image is worth 16x16 words: Transformers for image recognition at scale. *arXiv preprint arXiv:2010.11929*.
- Gould, S., Fernando, B., Cherian, A., Anderson, P., Cruz, R. S., and Guo, E. (2016). On differentiating parameterized argmin and argmax problems with application to bi-level optimization. *arXiv preprint arXiv:1607.05447*.
- Gould, S., Hartley, R., and Campbell, D. (2019). Deep declarative networks: A new hope. *arXiv preprint arXiv:1909.04866*.

- Griewank, A. and Walther, A. (2008). *Evaluating derivatives: principles and techniques of algorithmic differentiation*. SIAM.
- Guo, M.-H., Cai, J.-X., Liu, Z.-N., Mu, T.-J., Martin, R. R., and Hu, S.-M. (2021). Pct: Point cloud transformer. *Computational Visual Media*, 7(2):187–199.
- He, K., Zhang, X., Ren, S., and Sun, J. (2016). Deep residual learning for image recognition. In *Proceedings of the IEEE conference on computer vision and pattern recognition*, pages 770–778.
- Hein, M., Audibert, J.-Y., and Luxburg, U. v. (2007). Graph laplacians and their convergence on random neighborhood graphs. *Journal of Machine Learning Research*, 8(6).
- Jordan, R., Kinderlehrer, D., and Otto, F. (1998). The variational formulation of the fokker–planck equation. *SIAM journal on mathematical analysis*, 29(1):1–17.
- Kim, H., Papamakarios, G., and Mnih, A. (2021). The lipschitz constant of self-attention. In *International Conference on Machine Learning*, pages 5562–5571. PMLR.
- Kingma, D. P. and Ba, J. (2014). Adam: A method for stochastic optimization. *arXiv preprint arXiv:1412.6980*.
- Krantz, S. G. and Parks, H. R. (2012). *The implicit function theorem: history, theory, and applications*. Springer Science & Business Media.
- Lee, J., Lee, Y., Kim, J., Kosiorek, A., Choi, S., and Teh, Y. W. (2019). Set transformer: A framework for attention-based permutation-invariant neural networks. In *International Conference on Machine Learning*, pages 3744–3753. PMLR.
- Lu, Y., Zhong, A., Li, Q., and Dong, B. (2018). Beyond finite layer neural networks: Bridging deep architectures and numerical differential equations. In *International Conference on Machine Learning*, pages 3276–3285. PMLR.
- Luise, G., Rudi, A., Pontil, M., and Ciliberto, C. (2018). Differential properties of sinkhorn approximation for learning with wasserstein distance. *arXiv preprint arXiv:1805.11897*.
- Maas, A. L., Daly, R. E., Pham, P. T., Huang, D., Ng, A. Y., and Potts, C. (2011). Learning word vectors for sentiment analysis. In *Proceedings of the 49th Annual Meeting of the Association for Computational Linguistics: Human Language Technologies*, pages 142–150, Portland, Oregon, USA. Association for Computational Linguistics.
- Marshall, N. F. and Coifman, R. R. (2019). Manifold learning with bi-stochastic kernels. *IMA Journal of Applied Mathematics*, 84(3):455–482.
- Mialon, G., Chen, D., d’Aspremont, A., and Mairal, J. (2021). A trainable optimal transport embedding for feature aggregation and its relationship to attention. In *ICLR 2021-The Ninth International Conference on Learning Representations*.
- Milanfar, P. (2013). Symmetrizing smoothing filters. *SIAM Journal on Imaging Sciences*, 6(1):263–284.
- Niculae, V., Martins, A., Blondel, M., and Cardie, C. (2018). Sparsemap: Differentiable sparse structured inference. In *International Conference on Machine Learning*, pages 3799–3808. PMLR.
- Ott, M., Edunov, S., Baevski, A., Fan, A., Gross, S., Ng, N., Grangier, D., and Auli, M. (2019). fairseq: A fast, extensible toolkit for sequence modeling. In *Proceedings of NAACL-HLT 2019: Demonstrations*.
- Papineni, K., Roukos, S., Ward, T., and Zhu, W.-J. (2002). Bleu: a method for automatic evaluation of machine translation. In *Proceedings of the 40th annual meeting of the Association for Computational Linguistics*, pages 311–318.
- Paszke, A., Gross, S., Chintala, S., Chanan, G., Yang, E., DeVito, Z., Lin, Z., Desmaison, A., Antiga, L., and Lerer, A. (2017). Automatic differentiation in pytorch.
- Peng, C., Zhang, X., Yu, G., Luo, G., and Sun, J. (2017). Large kernel matters—improve semantic segmentation by global convolutional network. In *Proceedings of the IEEE conference on computer vision and pattern recognition*, pages 4353–4361.
- Peyré, G., Cuturi, M., et al. (2019). Computational optimal transport: With applications to data science. *Foundations and Trends® in Machine Learning*, 11(5-6):355–607.
- Radford, A., Wu, J., Child, R., Luan, D., Amodei, D., Sutskever, I., et al. (2019). Language models are unsupervised multitask learners. *OpenAI blog*, 1(8):9.
- Renardy, M. and Rogers, R. C. (2006). *An introduction to partial differential equations*, volume 13. Springer Science & Business Media.
- Ruder, S. (2016). An overview of gradient descent optimization algorithms. *arXiv preprint arXiv:1609.04747*.
- Ruthotto, L. and Haber, E. (2019). Deep neural networks motivated by partial differential equations. *Journal of Mathematical Imaging and Vision*, pages 1–13.
- Sander, M. E., Ablin, P., Blondel, M., and Peyré, G. (2021). Momentum residual neural networks. In *Proceedings of the 38th International Conference on Machine Learning*, volume 139 of *Proceedings of Machine Learning Research*, pages 9276–9287. PMLR.

- Santambrogio, F. (2017). {Euclidean, metric, and Wasserstein} gradient flows: an overview. *Bulletin of Mathematical Sciences*, 7(1):87–154.
- Singer, A. (2006). From graph to manifold laplacian: The convergence rate. *Applied and Computational Harmonic Analysis*, 21(1):128–134.
- Sinkhorn, R. (1964). A relationship between arbitrary positive matrices and doubly stochastic matrices. *The annals of mathematical statistics*, 35(2):876–879.
- Song, M., Montanari, A., and Nguyen, P. (2018). A mean field view of the landscape of two-layers neural networks. *Proceedings of the National Academy of Sciences*, 115:E7665–E7671.
- Sun, Q., Tao, Y., and Du, Q. (2018). Stochastic training of residual networks: a differential equation viewpoint. *arXiv preprint arXiv:1812.00174*.
- Tay, Y., Bahri, D., Yang, L., Metzler, D., and Juan, D.-C. (2020). Sparse sinkhorn attention. In *International Conference on Machine Learning*, pages 9438–9447. PMLR.
- Teh, Y., Doucet, A., and Dupont, E. (2019). Augmented neural odes. *Advances in Neural Information Processing Systems 32 (NIPS 2019)*, 32(2019).
- Tierney, L., Kass, R. E., and Kadane, J. B. (1989). Fully exponential laplace approximations to expectations and variances of nonpositive functions. *Journal of the american statistical association*, 84(407):710–716.
- Ting, D., Huang, L., and Jordan, M. (2011). An analysis of the convergence of graph laplacians. *arXiv preprint arXiv:1101.5435*.
- Vaswani, A., Shazeer, N., Parmar, N., Uszkoreit, J., Jones, L., Gomez, A. N., Kaiser, L., and Polosukhin, I. (2017). Attention is all you need. In *Advances in neural information processing systems*, pages 5998–6008.
- Vuckovic, J., Baratin, A., and Combes, R. T. d. (2021). On the regularity of attention. *arXiv preprint arXiv:2102.05628*.
- Wang, L., Ye, J., Zhao, Y., Wu, W., Li, A., Song, S. L., Xu, Z., and Kraska, T. (2018). Superneurons: Dynamic gpu memory management for training deep neural networks. In *Proceedings of the 23rd ACM SIGPLAN Symposium on Principles and Practice of Parallel Programming*, pages 41–53.
- Weinan, E. (2017). A proposal on machine learning via dynamical systems. *Communications in Mathematics and Statistics*, 5(1):1–11.
- Weinan, E., Han, J., and Li, Q. (2019). A mean-field optimal control formulation of deep learning. *Research in the Mathematical Sciences*, 6(1):10.
- Wolf, T., Debut, L., Sanh, V., Chaumond, J., Delangue, C., Moi, A., Cistac, P., Rault, T., Louf, R., Funtowicz, M., et al. (2019). Huggingface’s transformers: State-of-the-art natural language processing. *arXiv preprint arXiv:1910.03771*.
- Wormell, C. L. and Reich, S. (2021). Spectral convergence of diffusion maps: Improved error bounds and an alternative normalization. *SIAM Journal on Numerical Analysis*, 59(3):1687–1734.
- Wu, Z., Song, S., Khosla, A., Yu, F., Zhang, L., Tang, X., and Xiao, J. (2015). 3d shapenets: A deep representation for volumetric shapes. In *Proceedings of the IEEE conference on computer vision and pattern recognition*, pages 1912–1920.
- Yun, C., Bhojanapalli, S., Rawat, A. S., Reddi, S. J., and Kumar, S. (2019). Are transformers universal approximators of sequence-to-sequence functions? *arXiv preprint arXiv:1912.10077*.
- Zhai, X., Kolesnikov, A., Houlsby, N., and Beyer, L. (2021). Scaling vision transformers. *arXiv preprint arXiv:2106.04560*.
- Zhao, H., Jiang, L., Jia, J., Torr, P., and Koltun, V. (2020). Point transformer. *arXiv preprint arXiv:2012.09164*.
- Zhu, J.-Y., Park, T., Isola, P., and Efros, A. A. (2017). Unpaired image-to-image translation using cycle-consistent adversarial networks. In *Proceedings of the IEEE international conference on computer vision*, pages 2223–2232.
- Zweig, A. and Bruna, J. (2021). A functional perspective on learning symmetric functions with neural networks. In *International Conference on Machine Learning*, pages 13023–13032. PMLR.

Appendix

In Section A we give the proofs of all the Propositions and the Theorem. In Section B we present the implementation details of Sinkformers. Section C gives details for the experiments in the paper.

A Proofs

A.1 Invariance to the cost function - Proof of Proposition 1

Proof. We use the variational formulation for Sinkhorn (Peyré et al., 2019):

$$\text{Sinkhorn}(C) = \operatorname{argmin}_{K \mathbf{1}_n = K^\top \mathbf{1}_n = \mathbf{1}_n} \text{KL}(K|K^0)$$

with

$$\text{KL}(K|K^0) = \sum_{i,j} K_{i,j} \log\left(\frac{K_{i,j}}{K_{i,j}^0}\right),$$

where $K_{i,j}^0 = \exp(C_{i,j})$.

We let $\tilde{C}_{i,j} = C_{i,j} + f_i + g_j$. We have for $K \in U := \{K|K \mathbf{1}_n = K^\top \mathbf{1}_n = \mathbf{1}_n\}$ that $\text{KL}(K|e^{\tilde{C}}) = \sum_{i,j} K_{i,j} \log\left(\frac{K_{i,j}}{e^{C_{i,j} + f_i + g_j}}\right)$. This gives

$$\text{KL}(K|e^{\tilde{C}}) = \sum_{i,j} K_{i,j} [\log\left(\frac{K_{i,j}}{e^{C_{i,j}}}\right) - f_i - g_j] = \sum_{i,j} K_{i,j} [\log\left(\frac{K_{i,j}}{e^{C_{i,j}}}\right)] - \sum_i f_i - \sum_j g_j$$

so that

$$\text{KL}(K|e^{\tilde{C}}) = \text{KL}(K|e^C) - \sum_i f_i - \sum_j g_j.$$

This shows that $\text{KL}(K|e^{\tilde{C}})$ and $\text{KL}(K|e^C)$ have the same argmin on U which implies that $\text{Sinkhorn}(C) = \text{Sinkhorn}(\tilde{C})$. □

A.2 PDEs associated with $\mathbf{k}^0, \mathbf{k}^1, \mathbf{k}^\infty$ - Proof of Proposition 2

Proof. Recall that for $p \in \{0, 1, \infty\}$, we have $T_\mu^p(x) = \int k^p(x, x') W_V x' d\mu(x')$.

For $h \in \mathcal{C}(\mathbb{R}^d \times \mathbb{R}^d)$ consider

$$\mathcal{H}(\mu) = \int h(x, y) d\mu(x) d\mu(y).$$

Then we have (Santambrogio, 2017)

$$\frac{\delta \mathcal{H}}{\delta \mu}(\mu) = \int (h(x, \cdot) + h(\cdot, x)) d\mu(x).$$

We can now derive the different gradient expressions for T_μ^0 , T_μ^1 and T_μ^∞ .

For T_μ^0 : under Assumption 1, we have that $f(x, x') = e^{C(x, x')}$ is symmetric. This gives

$$\frac{\delta \mathcal{F}}{\delta \mu}(\mu) = \int f(\cdot, x') d\mu(x')$$

and by differentiation under the integral, under sufficient regularity assumptions on μ , this gives

$$\nabla_W(\mathcal{F}^0)(x) = \int \nabla_x f(x, x') d\mu(x') = \int f(x, x') \nabla_x c(x, x') d\mu(x').$$

Since $\nabla_x c(x, x') = -W_V x'$, we get

$$\nabla_W(\mathcal{F}^0)(x) = - \int e^{C(x, x')} W_V x' d\mu(x').$$

For $\mu = \frac{1}{n} \sum_{i=1}^n \delta_{x_i}$ this is exactly

$$\nabla_W(\mathcal{F}^0)(x) = - \sum_{j=1}^n K_{i,j}^0 W_V x_j.$$

For T_μ^1 : we have

$$\nabla[\log(\int e^{c(\cdot, x')} d\mu(x'))](x) = \int \frac{\nabla_x c(x, x') e^{c(x, x')}}{\int e^{c(x, y)} d\mu(y)} d\mu(x') = - \int \frac{e^{c(x, x')} W_V x'}{\int e^{c(x, y)} d\mu(y)} d\mu(x').$$

For T_μ^2 : one has the dual formulation for \mathcal{F}^∞ (Peyré et al., 2019):

$$2\mathcal{F}^\infty(\mu) = -\max_f \int_{\mathbb{R}^d} (f + f^c) d\mu \quad (8)$$

where we denote the soft c transform as

$$f^c(x') := -\log\left(\int e^{f(x)+c(x, x')} d\mu(x)\right), \quad (9)$$

which actually depends on μ and c . One has for an optimal pair $f = f^c$ (Peyré et al., 2019). In addition, one has $k^\infty(x, x') = e^{c(x, x') + f(x) + f(x')}$. The Wasserstein gradient of \mathcal{F}^∞ is then

$$\nabla_W \mathcal{F}^\infty(\mu) = -\nabla f$$

where f is an optimal solution of (8) (which is unique up to a constant). The gradient of f can be obtained using (9) and the fact that $f = f^c$:

$$\nabla f(x) = - \int e^{f(x)+f(x')+c(x, x')} \nabla_x c(x, x') d\mu(x') = - \int k^\infty(x, x') \nabla_x c(x, x') d\mu(x').$$

This finally gives

$$\nabla_W \mathcal{F}^\infty(\mu) : x \mapsto - \int k^\infty(x, x') W_V x' d\mu(x'),$$

that is what we wanted to show. \square

A.3 The SoftMax normalization does not correspond to a gradient flow - Proof of Proposition 3

Proof. Suppose by contradiction that $T_\mu^1 = -\nabla[\log(\int k^0(\cdot, x') d\mu(x'))]$ is a Wasserstein gradient. This implies that there exists a function F such that, $\forall \mu \in \mathcal{M}(\mathbb{R}^d)$ and $\forall x \in \mathbb{R}^d$,

$$\frac{\delta F}{\delta \mu}(\mu)(x) = \log(\int k^0(\cdot, x') d\mu(x')).$$

We therefore have

$$\frac{\delta^2 F}{\delta \mu^2}(\mu)(x, x') = \frac{k^0(x, x')}{\int k^0(x, y) d\mu(y)},$$

$\forall x, x' \in \mathbb{R}^d$. However, $\frac{\delta^2 F}{\delta \mu^2}(\mu)$ is symmetric for all $\mu \in \mathcal{M}(\mathbb{R}^d)$. The relationship $\frac{\delta^2 F}{\delta \mu^2}(\mu)(x, x') = \frac{\delta^2 F}{\delta \mu^2}(\mu)(x', x)$ then implies that for all μ, x and x' such that $k^0(x, x') \neq 0$ we have

$$\int k^0(x, y) d\mu(y) = \int k^0(x', y) d\mu(y).$$

Taking $\mu = \delta_y$ gives $k^0(x, y) = k^0(x', y)$, which by symmetry implies that k^0 is a constant.

This is a contradiction since $k^0(x, x') = \exp(x^\top W_Q^\top W_K x')$. \square

A.4 Sinkformer's PDE - Proof of Theorem 1

Proof. Since $W_Q^\top W_K$ is positive-definite we write it $W_Q^\top W_K = A^2$ where A is positive-definite. Note that thanks to Proposition 1, if $\kappa_\varepsilon(x, x') = \exp(-\frac{\|x-x'\|^2}{2\varepsilon})$, one has under Assumption 1 that $\kappa_\varepsilon^\infty(Ax, Ax') = k_\varepsilon^\infty(x, x')$. For $x \in \mathbb{R}^d$, we have

$$\bar{T}_{\mu,\varepsilon}^\infty(A^{-1}x) = \frac{1}{\varepsilon} \left(\int \kappa_\varepsilon^\infty(x, Ax') W_V x' \rho(x') dx' - W_V A^{-1}x \right).$$

We perform the change of variable $y = Ax'$. This gives

$$\bar{T}_{\mu,\varepsilon}^\infty(A^{-1}x) = \frac{1}{\varepsilon} \left(\int \kappa_\varepsilon^\infty(x, y) W_V A^{-1}y \rho(A^{-1}y) C_A dy - W_V A^{-1}x \right),$$

where C_A depends only on A . We then apply Theorem 1 from Marshall and Coifman (2019) with $f = W_V A^{-1}$, $q(x) = \rho(A^{-1}x)$ and $w = \frac{1}{C_A}$, to obtain that

$$\bar{T}_{\mu,\varepsilon}^\infty(A^{-1}\cdot) \rightarrow \frac{2\nabla f \nabla(q^{1/2})}{q^{1/2}} = W_V A^{-1} \frac{\nabla q}{q}$$

in L^2 norm. Since $q(x) = \rho(A^{-1}x)$ we have obtained that $\frac{\nabla q}{q} = A^{-1} \frac{\nabla \rho}{\rho}(A^{-1}\cdot)$ so that

$$\bar{T}_{\mu,\varepsilon}^\infty(A^{-1}x) \rightarrow W_V A^{-2} \frac{\nabla \rho}{\rho}(A^{-1}x) = W_V (W_Q^\top W_K)^{-1} \frac{\nabla \rho}{\rho}(A^{-1}x).$$

In other words,

$$\bar{T}_{\mu,\varepsilon}^\infty \rightarrow W_V (W_Q^\top W_K)^{-1} \frac{\nabla \rho}{\rho},$$

which is exactly what we wanted to show. Note that when $W_V = -W_Q^\top W_K$ this gives the expected result. The general form for the PDE is then

$$\partial_t \rho = \operatorname{div}(-W_V (W_Q^\top W_K)^{-1} \frac{\nabla \rho}{\rho} \times \rho)$$

which gives

$$\partial_t \rho = \Delta \rho$$

if $W_V = -W_Q^\top W_K$. □

A.5 Transformer's PDE - Proof of Proposition 4

Proof. Let $x \in \mathbb{R}^d$ and consider

$$g_\varepsilon(x) = \varepsilon T_{\mu,\varepsilon}^1(W_Q^{-1}x) = \frac{\int e^{-\frac{\|x-W_K x'\|^2}{2\varepsilon}} W_V x' \rho(x') dx'}{\int e^{-\frac{\|x-W_K x'\|^2}{2\varepsilon}} \rho(x') dx'}.$$

We perform the change of variable $y = W_K x'$. This gives:

$$g_\varepsilon(x) = \frac{\int e^{-\frac{\|x-y\|^2}{2\varepsilon}} W_V W_K^{-1}y \rho(W_K^{-1}y) dy}{\int e^{-\frac{\|x-y'\|^2}{2\varepsilon}} \rho(W_K^{-1}y) dy}.$$

Using the Laplace expansion result from Singer (2006), we obtain that

$$g_\varepsilon(x) = W_V W_K^{-1} \frac{x \rho(W_K^{-1}x) + \frac{\varepsilon}{2} \Delta(x \rho(W_K^{-1}x)) + o(\varepsilon)}{\rho(W_K^{-1}x) + \frac{\varepsilon}{2} \Delta(\rho(W_K^{-1}x)) + o(\varepsilon)}.$$

By doing a Taylor expansion for the denominator, we find

$$g_\varepsilon(x) = W_V W_K^{-1} \left(x + \frac{\varepsilon}{2} \frac{\Delta(x \rho(W_K^{-1}x))}{\rho(W_K^{-1}x)} + o(\varepsilon) \right) \left(1 - \frac{\varepsilon}{2} \frac{\Delta(\rho(W_K^{-1}x))}{\rho(W_K^{-1}x)} + o(\varepsilon) \right)$$

and

$$g_\varepsilon(x) = W_V W_K^{-1} (x + \varepsilon \frac{\nabla(\rho(W_K^{-1}x))}{\rho(W_K^{-1}x)} + o(\varepsilon).)$$

Since $\bar{T}_{\mu,\varepsilon}^1 = T_{\mu,\varepsilon}^1 + \frac{1}{\varepsilon} W_Q^\top W_Q = \frac{1}{\varepsilon} (g_\varepsilon(W_Q x) + W_Q^\top W_Q x)$ and because $W_V W_K^{-1} = -W_Q^\top W_K W_K^{-1} = -W_Q^\top$ we have

$$\bar{T}_{\mu,\varepsilon}^1 = -W_Q^\top W_K^{-1} \frac{\nabla \rho(W_K^{-1} W_Q x)}{\rho(W_K^{-1} W_Q x)} + o(1)$$

which is exactly the expected result. \square

B Implementation details

We implement Sinkhorn’s algorithm in log domain for stability. Given a matrix $K^0 \in \mathbb{R}^{n \times n}$ such that $K_{i,j}^0 = e^{C_{i,j}}$ for some $C \in \mathbb{R}^{n \times n}$, Sinkhorn’s algorithm (3) approaches $(f, g) \in \mathbb{R}^n \times \mathbb{R}^n$ such that $K^\infty = \text{diag}(e^{f^\infty}) K^0 \text{diag}(e^{g^\infty})$ by iterating in log domain, starting from $g^0 = \mathbb{0}_n$,

$$\begin{aligned} f^{l+1} &= \log(\mathbb{1}_n/n) - \log(K e^{g^l}) \quad \text{if } l \text{ is even} \\ g^{l+1} &= \log(\mathbb{1}_n/n) - \log(K^\top e^{f^l}) \quad \text{if } l \text{ is odd.} \end{aligned}$$

This allows for fast and accurate computations, where $\log(K e^{g^l})$ and $\log(K^\top e^{f^l})$ are computed using `log-sum-exp`.

C Experimental details

C.1 ModelNet 40 classification

Set Transformers. For our experiments on ModelNet using Set Transformers, we first preprocess the ModelNet 40 dataset. We then uniformly sample 5000 points from each element in the dataset. Our architecture is composed of two ISAB layers in the encoder and a decoder composed of a SAB and a Pooling by Multihead Attention (PMA) module. For the training, we use a batch-size of 64 and we use Adam (Kingma and Ba, 2014). The training is done over 300 epochs. The initial learning rate is 10^{-3} and is decayed by a factor 10 after 200 epochs.

Point Cloud Transformers. For our experiments on ModelNet using Point Clouds Transformers, we uniformly sample 1024 points from each element in the dataset. For the training, we use a batch-size of 32 and we use SGD (Ruder, 2016). The training is done over 300 epochs. The initial learning rate is 10^{-4} and is decayed by a factor 10 after 250 epochs.

C.2 Sentiment Analysis

We use the code available at the repository `nlp-tutorial`¹, where a pretrained Transformer is fine-tuned on the IMDB dataset. In our experiment, we reset the parameters of the pretrained Transformer and train it from scratch on the IMDB dataset. We use an architecture of depth 6, with 8 heads. For the training, we use a batch-size of 32 and we use Adam. The training is done over 15 epochs. The initial learning rate is 10^{-4} and is decayed by a factor 10 after 12 epochs.

C.3 Neural Machine Translation

We use the Transformer from `fairseq` and the command for training it on the IWSLT’14² dataset. When fine-tuning a Sinkformer, we simply divide the original learning rate by 10.

¹<https://github.com/lyeoni/nlp-tutorial/tree/master/text-classification-transformer>

²<https://github.com/pytorch/fairseq/blob/main/examples/translation/README.md>

C.4 Vision Transformers

Cats and dogs classification. This experiment is done on the cats and dogs³ dataset. For this experiment, we use a batch-size of 64 and Adam. We use an architecture of depth 6, with 8 heads, and select a patch-size of 16. The training is done over 300 epochs. The initial learning rate is 5×10^{-5} and divided by 10 after 250 epochs.

Impact of the patch size on the final accuracy. For this experiment, we use a batch-size of 100 and Adam. We use an architecture of depth 1, with 1 heads, without non-linearity, and select different values for the patch-size. The training is done over 45 epochs. The initial learning rate is 1×10^{-3} (resp. 2×10^{-3}) for the Transformer (resp. Sinkformer) and divided by 10 after 35 epochs and again by 10 after 41 epochs.

³<https://www.kaggle.com/c/dogs-vs-cats/data>